

# Nuclear Magnetic Resonance Studies of the Formation of Tertiary Alkyl Complexes of Iron(III) Porphyrins and Their Reactions with Dioxygen

Alan L. Balch,<sup>\*,†</sup> Rebecca L. Hart,<sup>†</sup> Lechosław Latos-Grażyński,<sup>‡</sup> and Teddy G. Traylor<sup>§</sup>

Contribution from the Departments of Chemistry, The University of California, Davis, California 95616, University of Wrocław, Poland, and The University of California, San Diego, California 92093. Received February 2, 1990

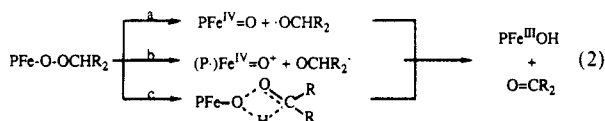
**Abstract:** Iron(III) complexes of tetra-(*p*-tolyl)porphyrin (TPPH<sub>2</sub>) with axial adamantyl (1-ad), camphane (4-cam), and *tert*-butyl ligands have been prepared and characterized by NMR spectroscopy. These have typical properties for low-spin ( $S = 1/2$ ), five-coordinate complexes. Analyses of the paramagnetic NMR spectral patterns for a variety of axial ligands are made and compared with those of aliphatic amines. These spectra exhibit sizeable dipolar shifts and can show non-Curie temperature dependence, particularly for the  $\beta$ -protons. Treatment of TTPFe<sup>III</sup>(4-cam), TTPFe<sup>III</sup>(1-ad), or TTPFe<sup>III</sup>(*t*-Bu) with dioxygen in toluene at  $-70$  °C produces a mixture of TTPFe<sup>III</sup>OH, TTPFe<sup>III</sup>OFe<sup>III</sup>TTP, and TTPFe<sup>III</sup>OOOR (R = *tert*-butyl, 4-cam, or 1-ad). The absence of hydrogen atoms in the  $\alpha$ -carbon of these tertiary alkyl peroxide complexes alters their reactivity so that an intermediate formed by the O–O bond-breaking step can be detected. Treatment of TTPFe<sup>III</sup>OO(4-cam) with pyridine at  $-70$  °C results in its conversion into TTPFe<sup>IV</sup>=O through homolysis of the O–O bond.

The insertion of dioxygen into Fe–C bonds of the low spin ( $S = 1/2$ ) alkyl iron(III) porphyrin complexes (eq 1)<sup>1</sup> presents a method of generating the highly reactive, high-spin ( $S = 5/2$ ) alkyl peroxide complexes in a nonpolar environment at low temperatures.<sup>1–3</sup> This has allowed these much discussed intermediates



to be subject to direct NMR spectroscopic observation. The behavior of these alkyl peroxide complexes is of interest in regard to the mode of action of a number of enzymes (e.g., peroxidases,<sup>4–6</sup> lipoxygenases,<sup>7,8</sup> steroidal aromatases<sup>9,10</sup>) and the mechanism of O–O bond cleavage in iron-catalyzed reactions of peroxides.<sup>11–19</sup>

For alkyl peroxide complexes bearing a hydrogen on the  $\alpha$ -carbon of the alkyl group, thermal decomposition could involve the homolytic (a), heterolytic (b), or concerted (c) paths shown in eq 2. This reaction rapidly yields the carbonyl compound and



the iron(III) product without producing intermediates in quantities suitable for detection by NMR spectroscopy.<sup>3</sup> We suspected that if the  $\alpha$ -hydrogen were not present, the course of decomposition could be sufficiently altered so that the intermediates formed by paths a or b might be detected. However, our initial attempts to prepare the requisite iron tertiary alkyl complexes with either *tert*-butyl or trifluoromethyl substituents did not produce the desired compounds.<sup>3</sup>

In an alternate experiment, the reaction of *tert*-butyl hydroperoxide with TMPFe<sup>III</sup>OH in toluene solution at  $-80$  °C was shown to produce the reactive intermediate, TMPFe<sup>III</sup>OObut.<sup>20</sup> Upon warming or treatment with an amine (B) this was converted into the five- or six-coordinate ferryl complexes,<sup>21</sup> TMPFe<sup>IV</sup>=O or (B)TMPFe<sup>IV</sup>O, respectively. This observation strongly suggests that homolysis has occurred. However, the possibility that heterolysis followed by reaction of the [(P<sup>•</sup>)Fe<sup>IV</sup>=O]<sup>+</sup> with *tert*-butyl

hydroperoxide might have resulted in the formation of PFe<sup>IV</sup>=O allowed for some ambiguity in the interpretation.

Here we report new efforts to obtain 15-electron iron(III) porphyrin complexes bearing tertiary alkyl substituents and their reactivity with dioxygen. We describe a reinvestigation of the reaction of TTPFe<sup>III</sup>Cl with *tert*-butyl magnesium bromide and show that the *tert*-butyl complex can be observed at low temperatures, and we demonstrate that complexes with the constrained alkyl groups 1-adamantyl (1-ad) and 4-camphyl (4,7,7-trimethylbicyclo[2.2.1]heptane),<sup>22</sup> which are shown in Figure 1, can be formed. Our rationale for the use of the 4-camphyl group to stabilize the Fe–C bond is as follows.

Within a series of bridgehead radicals, the stability decreases as the *s*-character of the radical increases; this increase is brought

- (1) Arasasingham, R. D.; Balch, A. L.; Latos-Grażyński, L. *J. Am. Chem. Soc.* **1987**, *109*, 5846.
- (2) Arasasingham, R. D.; Balch, A. L.; Latos-Grażyński, L. In *Studies in Organic Chemistry*; Ando, W., Moro-oka, Y., Eds.; Elsevier: Amsterdam, The Netherlands, 1987; Vol. 33, p 417.
- (3) Arasasingham, R. D.; Balch, A. L.; Cornman, C. R.; Latos-Grażyński, L. *J. Am. Chem. Soc.* **1989**, *111*, 4357.
- (4) Dunford, H. B.; Stillman, J. S. *Coord. Chem. Rev.* **1976**, *19*, 187.
- (5) Hewson, W. D.; Hager, L. P. In *The Porphyrins*; Dolphin, D., Ed.; Academic Press: New York, 1979; Vol. 7, p 295.
- (6) Marnett, L. J.; Weller, P.; Battista, J. R. In *Cytochrome P450: Structure, Mechanism and Biochemistry*; Ortiz de Montellano, P. R., Ed.; Plenum Press: New York, 1986; p 29.
- (7) Aust, S. D.; Svingen, B. A. *Free Radicals in Biology* **1982**, *5*, 1.
- (8) Vliegthart, J. F. G.; Veldink, G. A. *Free Radicals in Biology* **1982**, *5*, 29.
- (9) Stevenson, D. E.; Wright, J. N.; Akhtar, M. *J. Chem. Soc., Chem. Commun.* **1985**, 1078.
- (10) Cole, P. A.; Robinson, C. H. *J. Am. Chem. Soc.* **1988**, *110*, 1284.
- (11) Traylor, T. G.; Lee, W. A.; Stynes, D. V. *J. Am. Chem. Soc.* **1984**, *106*, 755.
- (12) Traylor, T. G.; Xu, F. *J. Am. Chem. Soc.* **1987**, *109*, 6201.
- (13) Groves, J. T.; Watanabe, Y. *J. Am. Chem. Soc.* **1986**, *108*, 7834.
- (14) Bruice, T. C.; Zipplies, M. F.; Lee, W. A. *Proc. Natl. Acad. Sci. U.S.A.* **1986**, *83*, 4646.
- (15) Lee, W. A.; Yuan, L.-C.; Bruice, T. C. *J. Am. Chem. Soc.* **1988**, *110*, 4277.
- (16) Balasubramanian, P. N.; Lindsay-Smith, J. R.; Davies, M. J.; Kaaret, T. W.; Bruice, T. C. *J. Am. Chem. Soc.* **1989**, *111*, 1477.
- (17) Labeque, R.; Marnett, L. J. *J. Am. Chem. Soc.* **1989**, *111*, 6621.
- (18) Labeque, R.; Marnett, L. J. *J. Am. Chem. Soc.* **1987**, *109*, 2828.
- (19) Labeque, R.; Marnett, L. J. *Biochemistry* **1988**, *27*, 7060.
- (20) Arasasingham, R. D.; Cornman, C. R.; Balch, A. L. *J. Am. Chem. Soc.* **1989**, *111*, 7800.
- (21) Balch, A. L.; Chan, Y. W.; Cheng, R. J.; La Mar, G. N.; Latos-Grażyński, L.; Renner, M. W. *J. Am. Chem. Soc.* **1984**, *106*, 7779.
- (22) Winstein, S.; Traylor, T. G. *J. Am. Chem. Soc.* **1956**, *78*, 2597.

<sup>†</sup> University of California, Davis.

<sup>‡</sup> University of Wrocław.

<sup>§</sup> University of California, San Diego.

<sup>1</sup> Abbreviations used: P, porphyrin dianion; P<sup>•</sup>, porphyrin radical monoanion; TPP, tetraphenylporphyrin; TTP, tetra-(*p*-tolyl)porphyrin dianion; TMP, tetramesityl porphyrin dianion; R, alkyl group or hydrogen; ad, adamantyl; cam, camphane; py, pyridine; B, amine base.

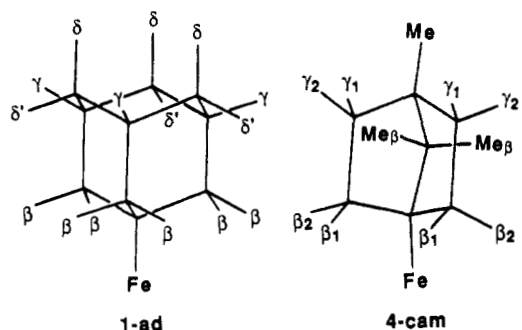
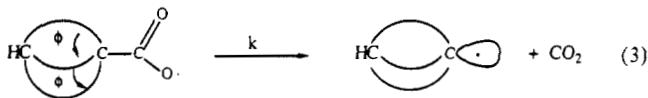


Figure 1. The 1-ad and 4-cam ligands.

about by decreasing the angles at the bridgehead.<sup>23,24</sup> Thus the rate of decarboxylation in eq 3 decreases as the angle,  $\phi$ , decreases, and the *s*-character, determined by  $^{13}\text{C}$ -H coupling at the bridgehead, increases. As a consequence, the lengths of bonds



to the bridgehead shorten, and the bond strength increases<sup>25</sup> as the *s*-character increases. Thus any bond to the 1-position in camphane (28% *s*-character) is expected to be stronger and shorter than the corresponding bond to the 1-position of adamantyl or to the *tert*-butyl group. We have therefore chosen the 1-camphyl group to improve the strength of the Fe-C bond in these systems. (Further improvement is expected for groups having still greater *s*-character, e.g., cyclopropyl and homocubyl groups.<sup>23,24</sup>)

Preparing these tertiary alkyl complexes with well-defined, rigid geometry also gave us the opportunity to explore the  $^1\text{H}$  NMR spectral properties of alkyl ligands in paramagnetic complexes. These show a number of novel features that include both upfield and downfield shifts for saturated groups and a 127-ppm shift (at  $-70^\circ\text{C}$ ) in the  $\beta$ -proton resonance on going from  $\text{TTPFe}^{\text{III}}(\text{C}_2\text{H}_5)$  ( $\beta$ -ethyl protons at  $-154$  ppm) to  $\text{TTPFe}^{\text{III}}(n\text{-C}_3\text{H}_7)$  ( $\beta$ -propyl protons at  $-27$  ppm).<sup>3,26,27</sup>

## Results

**NMR Characterization of the Tertiary and Other Alkyl Complexes of Iron(III) Porphyrins.**  $^1\text{H}$  NMR spectral data for a variety of  $\text{PFe}^{\text{III}}\text{R}$  complexes are collected in Table I. In all cases a pyrrole resonance at ca.  $-35$  ppm at  $-70^\circ\text{C}$  is observed. This is characteristic of the presence of a low spin ( $S = 1/2$ ) iron(III) porphyrin complex.<sup>3,26,27,28</sup> Figure 2 shows a plot of the temperature dependence of the  $^1\text{H}$  NMR chemical shifts for  $\text{TTPFe}^{\text{III}}(n\text{-Pr})$  and  $\text{TTPFe}^{\text{III}}(i\text{-Pr})$ , typical examples of complexes with primary and secondary alkyl substituents. Both show similar behavior for the pyrrole and phenyl resonances, and this behavior is characteristic of low-spin iron(III). However, the behavior of the alkyl resonances is unexpected. The plot of the  $\beta$ -protons for the *n*-propyl derivative shows a decreasing hyperfine shift with decreasing temperature, while all other protons of this and the isopropyl compound show increasing hyperfine shifts with decreasing temperature as the Curie law predicts.

Repeated attempts to prepare  $\text{TTPFe}^{\text{III}}(t\text{-Bu})$  under the conditions used to prepare the *n*-Pr and *i*-Pr derivatives have produced only  $\text{TTPFe}^{\text{II}}$ . We surmised that the  $\text{TTPFe}^{\text{II}}$  formed as a result

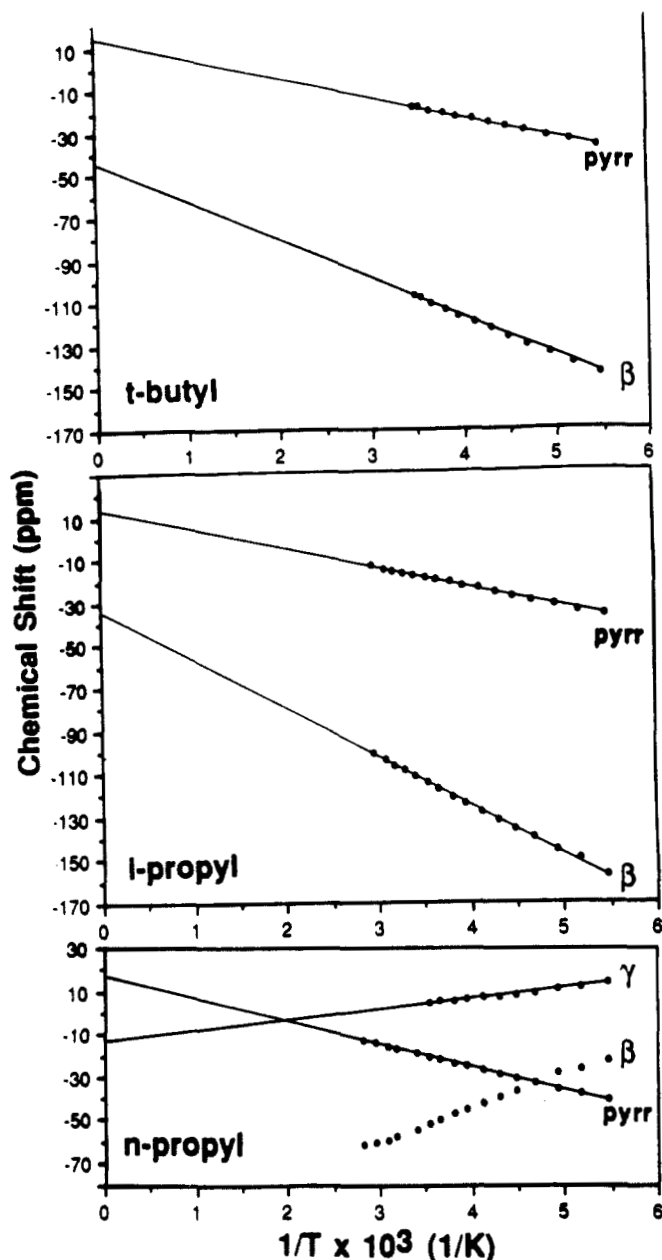


Figure 2. Temperature dependence of chemical shifts for  $\text{TTPFe}^{\text{III}}(n\text{-C}_3\text{H}_7)$ ,  $\text{TTPFe}^{\text{III}}(i\text{-C}_3\text{H}_7)$ , and  $\text{TTPFe}^{\text{III}}(t\text{-C}_4\text{H}_9)$  in toluene- $d_8$ . Solid lines show the extrapolation of the experimental data points as expected from the Curie law. The resonances of the  $\beta$  and  $\gamma$  protons on the alkyl group are designated  $\beta$  and  $\gamma$ , respectively, and the pyrrole protons are labeled pyrr.

of thermal decomposition (Fe-C homolysis) of  $\text{TTPFe}^{\text{III}}(t\text{-Bu})$  that was transiently produced. In order to search for  $\text{TTPFe}^{\text{III}}(t\text{-Bu})$  more carefully, we investigated the reaction between  $\text{TTPFe}^{\text{III}}\text{Cl}$  with *tert*-butyl magnesium chloride at  $-80^\circ\text{C}$  with direct  $^1\text{H}$  NMR observation immediately after mixing. Under these conditions, resonances due to  $\text{TTPFe}^{\text{III}}(t\text{-Bu})$  are readily observed (Table I, Figure 2). In particular the three, equivalent  $\beta$ -methyl groups are found at a characteristic high field position seen also for the ethyl and isopropyl derivatives.  $\text{TTPFe}^{\text{III}}(t\text{-Bu})$  can be detected while the sample is warmed to  $0^\circ\text{C}$  with some  $\text{TTPFe}^{\text{II}}$  present. However, warming above  $0^\circ\text{C}$  results in rapid decomposition to form  $\text{TTPFe}^{\text{II}}$ , so that the  $^1\text{H}$  NMR spectrum of the *t*-Bu derivative cannot be obtained at higher temperature.

Treatment of  $\text{TTPFe}^{\text{III}}\text{Cl}$  with the Grignard reagent derived from adamantyl bromide<sup>29</sup> yields a solution containing both

(23) Sieber, A.; Kriefer, H.; Traylor, T. G. *Interscience Chem. Reports* **1969**, *3*, 289.

(24) Kochi, J. In *Free Radicals*; Kochi, J., Ed.; John Wiley: New York, 1973; Vol. 2, p 700.

(25) Alden, R. A.; Kraut, J.; Traylor, T. G. *J. Am. Chem. Soc.* **1968**, *90*, 74.

(26) Lexa, D.; Mispelner, J.; Savéant, J.-M. *J. Am. Chem. Soc.* **1981**, *103*, 6806.

(27) Coccolios, P.; Lagrange, G.; Guillard, R. J. *Organomet. Chem.* **1983**, *253*, 65.

(28) La Mar, G. N.; Walker, F. A. *J. Am. Chem. Soc.* **1973**, *95*, 1782.

(29) Molle, G.; Bauer, P.; Dubois, J. E. *J. Org. Chem.* **1982**, *47*, 4120.

**Table I.**  $^1\text{H}$  NMR Data for Iron(III) Alkyl Complexes in Toluene- $d_6$ 

compd	$T$ ( $^{\circ}\text{C}$ )	pyrrole (ppm)	alkyl (ppm)		
			$\beta$	$\gamma$	$\delta$
TTPFe(Et)	-70	-34.0	-154.0		
	20	-18.4	-117.0		
TTPFe( <i>n</i> -Pr)	-70	-35.0	-27.4	12.0	
	20	-18.5	-54.3		
TTPFe( <i>i</i> -Pr)	-70	-32.6	-145.6		
	20	-18.2	-111.7		
TTPFe( <i>n</i> -Bu) <sup>a</sup>	20	-18.4	-63.7	18.2	10.3
TTPFe( <i>t</i> -Bu)	-70	-33.7	-135.5		
	0 <sup>b</sup>	-21.0	-111.5		
TTPFe(1-ad)	-70	-33.3	-17.9	-14.9	20.6, -27.1
	20	-18.4	-19.8	-14.4	10.3, -20.8
TTPFe(4-cam)	-70	-30.8	42.8, -48.7	44.3, 25.5	16.4, <sup>c</sup> -2.7 <sup>d</sup>
	20	-16.8	23.9, -39.9	27.8, 14.0	9.9, <sup>c</sup> 1.54 <sup>d</sup>

<sup>a</sup>Data from ref 23. <sup>b</sup>Highest temperature at which this species could be observed. <sup>c</sup> $\beta$ -methyl. <sup>d</sup>Methyl.

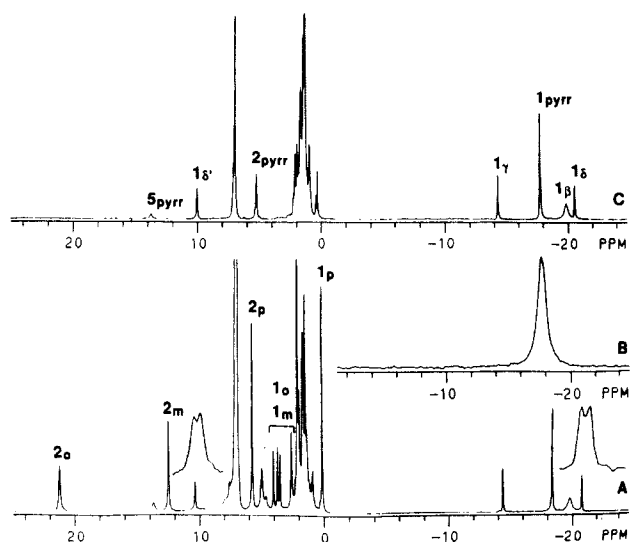


**Figure 3.** NMR spectra: (A) 360 MHz,  $^1\text{H}$  for TTPFe<sup>III</sup>(1-ad) at 21  $^{\circ}\text{C}$ ; insets show expansions of the doublets at 10.5 and -20.8 ppm; (B) 76 MHz,  $^2\text{H}$  for pyrrole- $d_5$ -TTPFe<sup>III</sup>(1-ad) at 25  $^{\circ}\text{C}$ ; (C) 360 MHz,  $^1\text{H}$  for *p*-tolyl- $d_{28}$ -TTPFe<sup>III</sup>(1-ad) at 25  $^{\circ}\text{C}$ . Resonances due to TTPFe<sup>III</sup>(1-ad) are labeled 1, those of TTPFe<sup>II</sup> are labeled 2, those of TTPFe<sup>III</sup>OFe<sup>III</sup>TTP are labeled 5. Subscripts refer to assignments: pyr, porphyrin pyrrole protons; o, m, p, *ortho*, *meta*, *para* porphyrin phenyl protons;  $\beta$ ,  $\gamma$ ,  $\delta$ ,  $\delta'$ , adamantyl  $\beta$ ,  $\gamma$ ,  $\delta$  and  $\delta'$ -protons.

TTPFe<sup>III</sup>(1-ad), 1(1-ad), and TTPFe<sup>II</sup>, 2. The  $^1\text{H}$  NMR spectrum of such a solution at 21  $^{\circ}\text{C}$  is shown in trace A of Figure 3. In the spectrum resonances due to TTPFe<sup>III</sup>(1-ad) are labeled 1, while those of TTPFe<sup>II</sup><sup>30</sup> and TTPFe<sup>III</sup>OFe<sup>III</sup>TTP,<sup>31</sup> which have been independently observed and fully assigned, are labeled 2 and 5, respectively. The assignment of the pyrrole resonance of 1(1-ad) was verified by  $^2\text{H}$  NMR spectroscopy of a sample prepared from (pyrrole- $d_5$ )-TPP. Inset B of Figure 3 shows the region of that spectrum from -10 to -24 ppm where the pyrrole resonance (not shown) at 5 ppm due to the pyrrole resonance of TTPFe<sup>II</sup>. The phenyl resonances of TTPFe<sup>III</sup>(1-ad) are assigned by comparison to the  $^1\text{H}$  NMR spectrum obtained from a sample prepared from (phenyl- $d_{28}$ )-TPP. That spectrum is shown in trace C of Figure 3. The *para* methyl resonance is readily assigned on the basis of its intensity, and the remaining four resonances in the 2-4 ppm region are due to the *ortho* and *meta* phenyl protons. When expanded, these peaks show doublet character due to the expected spin-spin coupling. Two of each type are expected since the two sides of the porphyrin plane are different, and rotation about the porphyrin-phenyl C-C bond is restricted. The re-

**Table II.** Relaxation Data

resonance	$T_1$ (ms)	resonance	$T_1$ (ms)
TTPFe <sup>III</sup> (1-ad) (-40 $^{\circ}\text{C}$ ) <sup>a</sup>			
pyrr	25.8	<i>p</i> -CH <sub>3</sub>	190.8
$\beta$	1.63	<i>m</i> <sub>1</sub>	133.5
$\gamma$	39.26	<i>m</i> <sub>2</sub>	114.1
$\delta'$ (15.3 ppm)	20.6	<i>o</i> <sub>1</sub>	50.2
$\delta$ (-24.1 ppm)	152.9	<i>o</i> <sub>2</sub>	89.6
TTPFe(4-cam) (-60 $^{\circ}\text{C}$ ) <sup>a</sup>			
pyrr	~20	$\beta_2$	~2
$\gamma_1$ (41.54 ppm)	13.3	Me $\beta$	4.91
$\gamma_2$		Me	43.6
$\beta_1$	~2		

<sup>a</sup>Temperatures selected to give optimal separation of individual resonances.

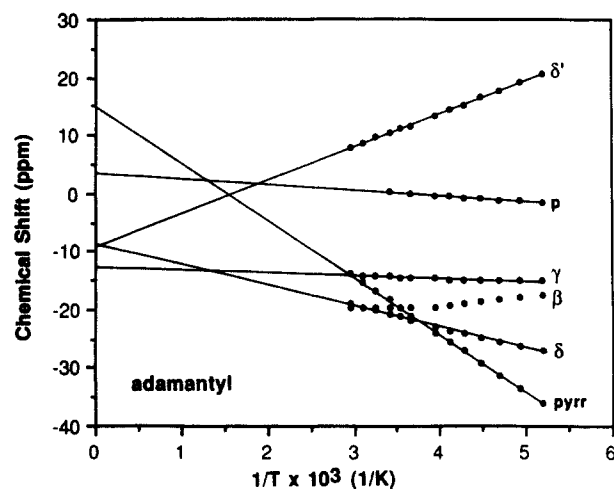


**Figure 4.** Temperature dependence of chemical shifts for TTPFe<sup>III</sup>(1-ad) in toluene- $d_6$ . Solid lines show the extrapolation of the experimental data points as expected from the Curie law. Labels follow those in Figure 3.

maining four resonances are due to the four adamantyl protons. On the basis of its intensity and line width, the resonance at -19.5 ppm is assigned to the  $\beta$ -protons, with their close proximity to the iron determining their width (vide infra). Two of the remaining three resonances are coupled to one another. The inserts to trace A show expansion of these two resonances. Decoupling experiments show that indeed it is these two resonances that are coupled with  $J(\text{H,H}) = 10$  Hz. The magnitude of this coupling is what is expected for geminal protons in a fused cyclohexane ring, and so these resonances are assigned to the  $\delta$  and  $\delta'$  protons.<sup>32</sup> However, at this stage of discussion specific identification of the most downfield resonance with either  $\delta$  or  $\delta'$  is not established. The remaining resonance at -14.2 ppm is then assigned to the three, equivalent  $\gamma$  protons. This assignment is consistent with 1-ad group retaining its intrinsic 3-fold symmetry. To do that, rotation about the Fe-C bond must be occurring.

The effect of temperature on the spectrum of TTPFe<sup>III</sup>(1-ad) is shown in Figure 4. While the pyrrole and phenyl resonances show behavior that is generally found for low-spin Fe(III) complexes,<sup>28</sup> the behavior of the 1-ad resonances is unusual. Notice also the peculiar slope and curvature for the  $\beta$ -proton resonance.

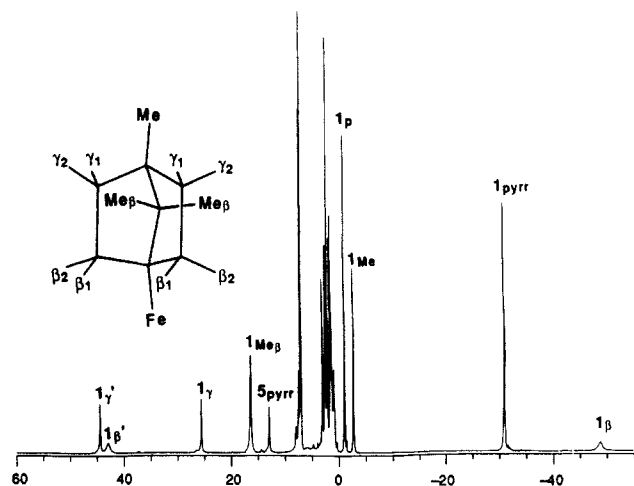
$T_1$  data for the protons in TTPFe<sup>III</sup>(1-ad) are collected along with those for other related compounds in Table II.

Figure 5 shows the  $^1\text{H}$  NMR spectrum of TTPFe<sup>III</sup>(4-cam) in toluene at -70  $^{\circ}\text{C}$  resulting from the reaction of TTPFe<sup>III</sup>Cl with Li(4-cam). Resonance assignments can be made by comparison with those of TTPFe<sup>III</sup>(1-ad). The pyrrole resonance appears at -31 ppm; its assignment has been confirmed by observing the  $^1\text{H}$  and  $^2\text{H}$  NMR spectra of the (pyrrole- $d_5$ )-TPP analogue. The alkyl

(30) Goff, H.; La Mar, G. N.; Reed, C. A. *J. Am. Chem. Soc.* **1977**, *99*, 3641.

(31) La Mar, G. N.; Eaton, G. R.; Holm, R. H.; Walker, F. A. *J. Am. Chem. Soc.* **1973**, *95*, 63.

(32) Silverstein, R. M.; Bassler, G. C.; Morrill, T. C. *Spectroscopic Identification of Organic Compounds*, 4th ed.; John Wiley and Sons: New York, 1981; p 209.



**Figure 5.** The 360-MHz  $^1\text{H}$  NMR spectrum of  $\text{TTPFe}^{\text{III}}(4\text{-cam})$  in toluene- $d_8$  at  $-70^\circ\text{C}$ . Resonances of this complex are labeled 1 with subscripts giving the individual proton assignments as done in Figure 3, along with the labeling of 4-cam.

resonances may be assigned on the basis of the line widths and intensities. The two broadest resonances, which have intensity 2 relative to the pyrrole peak of intensity 8, are assigned to the two types of  $\beta$  protons. The resonance at 19.4 ppm with relative intensity 6 is assigned to the protons of the two  $\beta$ -methyl groups, and the resonance at  $-6$  ppm with relative intensity 3 is assigned to the  $\gamma$ -methyl group. The remaining resonances at 44.5 and 25.5 ppm each of intensity 2 and similar line widths are assigned to the  $\gamma$  and  $\gamma'$  protons. Assignments of resonances  $\beta$  and  $\beta'$  ( $\gamma$  and  $\gamma'$ ) to specific locations  $\beta_1$  or  $\beta_2$  ( $\gamma_1$  or  $\gamma_2$ ) has not been made. The sample contains a negligible amount of  $\text{TTPFe}^{\text{II}}$  and does not contain a very small amount of  $\text{TTPFe}^{\text{III}}\text{OFe}^{\text{III}}\text{TTP}$ . Our experience in handling  $\text{TTPFe}^{\text{III}}(4\text{-cam})$  indicates that it is considerably more stable than  $\text{TTPFe}^{\text{III}}(1\text{-ad})$ , which is always found in combination with an appreciable quantity of  $\text{TTPFe}^{\text{II}}$ .

**Dioxygen Insertion.**  $\text{TTPFe}^{\text{III}}(t\text{-Bu})$ ,  $\text{TTPFe}^{\text{III}}(1\text{-ad})$ , and  $\text{TTPFe}^{\text{III}}(4\text{-cam})$  react readily with dioxygen at  $-70^\circ\text{C}$  in toluene solution to form alkyl peroxide complexes similar to those seen for the primary and secondary alkyl groups studied earlier.<sup>1-3</sup> The chemical shifts observed for the pyrrole and meta protons of these peroxocomplexes are as follows:  $\text{TTPFeOO}(t\text{-Bu})$ , 117.6 ppm (pyrr), 13.4, 11.8 meta (at  $-80^\circ\text{C}$ );  $\text{TTPFeOO}(1\text{-ad})$ , 116 (pyrr), 12.0, 13.2 meta (at  $-70^\circ\text{C}$ );  $\text{TTPFeOO}(4\text{-cam})$ , 106.7 (pyrr), 11.1, 12.4 meta (at  $-60^\circ\text{C}$ ). The observations on  $\text{TTPFeOO}(t\text{-Bu})$  obtained in this fashion are entirely consistent with previous work on the formation of  $\text{PFe}^{\text{III}}\text{OO}(t\text{-Bu})$  from *tert*-butyl hydroperoxide.<sup>20</sup> Since  $\text{TTPFe}^{\text{III}}(4\text{-cam})$  can be prepared in purer form without the presence of  $\text{TTPFe}^{\text{II}}$ , its reactions give the most conclusive data regarding the formation and cleavage of the alkylperoxo ligand.

Trace A of Figure 6 shows the  $^2\text{H}$  NMR spectrum of a sample of pyrrole- $d_8$ - $\text{TTPFe}^{\text{III}}(4\text{-cam})$  at  $-70^\circ\text{C}$  after exposure to dioxygen. (Trace C shows an expansion of this spectrum in the 30–0-ppm range.) Three prominent pyrrole resonances are present which are identified as 3,  $\text{TPPFe}^{\text{III}}\text{OO}(4\text{-cam})$ ; 4,  $\text{TPPFe}^{\text{III}}\text{OH}$ ; and 5,  $\text{TPPFe}^{\text{III}}\text{OFe}^{\text{III}}\text{TTP}$ . The resonances of  $\text{TPPFe}^{\text{III}}\text{OH}$  and  $\text{TPPFe}^{\text{III}}\text{OFe}^{\text{III}}\text{TTP}$  are identified by comparison with those of independently prepared samples.<sup>3</sup> As established previously, the pyrrole resonances of the alkyl peroxide complex occur at higher field (lower frequency) than that of the hydroxy complexes.<sup>3</sup> At this stage there is no evidence for the presence of the peroxo-bridged dimer,  $\text{TPPFe}^{\text{III}}\text{OFe}^{\text{III}}\text{TTP}$ . On warming (not shown) the pyrrole resonances of both  $\text{TPPFe}^{\text{III}}\text{OO}(4\text{-cam})$  and  $\text{TPPFe}^{\text{III}}\text{OH}$  decrease in intensity as the resonance of  $\text{TPPFe}^{\text{III}}\text{OFe}^{\text{III}}\text{TTP}$  grows. During warming, the pyrrole resonance of  $\text{TPPFe}^{\text{III}}\text{OO}(4\text{-cam})$  is lost more rapidly than that of  $\text{TPPFe}^{\text{III}}\text{OH}$  as found for primary and secondary alkyl peroxide complexes.<sup>3</sup>

Traces B and D of Figure 6 show the effect of addition of pyridine to this sample. The pyrrole resonance of  $\text{TPPFe}^{\text{III}}\text{OO}$

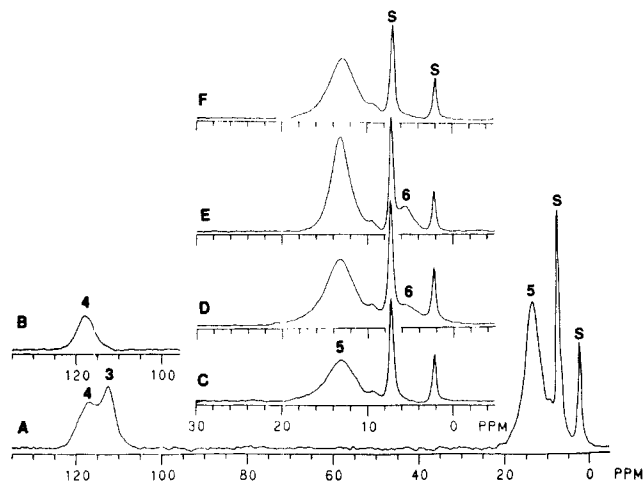


**Figure 6.** The 76-MHz  $^2\text{H}$  NMR spectra of a toluene solution of pyrrole- $d_8$ - $\text{TTPFe}^{\text{III}}(4\text{-cam})$ , after the addition of dioxygen at  $-70^\circ\text{C}$ : (A) and (C) (an expansion of the 30–0-ppm region), immediately after addition at  $-70^\circ\text{C}$ ; (B) and (D) after the addition of pyridine at  $-70^\circ\text{C}$ ; (E), as in (D) after warming to  $-50^\circ\text{C}$ ; (F) as in (E) after warming to  $25^\circ\text{C}$ , recoiling to  $-70^\circ\text{C}$  and recording at  $-70^\circ\text{C}$ . Pyrrole resonances are assigned as 3,  $\text{TTPFe}^{\text{III}}\text{OO}(4\text{-cam})$ ; 4,  $\text{TTPFe}^{\text{III}}\text{OH}$ ; 5,  $\text{TTPFe}^{\text{III}}\text{OFe}^{\text{III}}\text{TTP}$ ; 6, (py) $\text{TTPFe}^{\text{IV}}=\text{O}$ , S naturally occurring deuterated solvent.

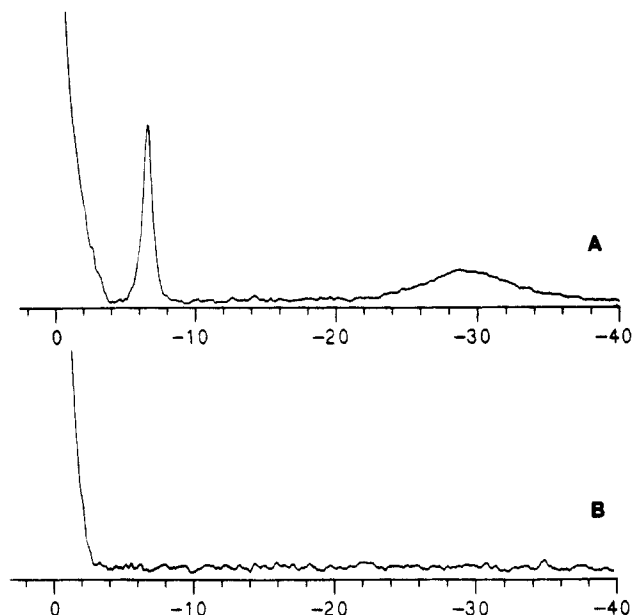


**Figure 7.** The 360-MHz  $^1\text{H}$  NMR spectra of a sample of  $\text{TTPFe}^{\text{III}}(4\text{-cam})$  in toluene- $d_8$  after the successive addition of dioxygen and pyridine (A) at  $-70^\circ\text{C}$  and (B) after warming to  $25^\circ\text{C}$ , recoiling, and recording at  $-70^\circ\text{C}$ .

(4-cam) has lost almost all of its intensity, while a new resonance at 6 ppm has grown. This resonance is better resolved when the sample is warmed to  $-50^\circ\text{C}$  as shown in trace E. The peaks of  $\text{TPPFe}^{\text{III}}\text{OH}$  and  $\text{TPPFe}^{\text{III}}\text{OFe}^{\text{III}}\text{TTP}$  remain prominent in the spectrum. The new resonance is readily identified as the pyrrole resonance from (py) $\text{TTPFe}^{\text{IV}}=\text{O}$ , 6.<sup>33,34</sup> On warming, the intensity of this resonance decreases as seen in previous work on this six-coordinate ferryl complex. Trace F shows a spectrum of this sample after it was warmed to  $25^\circ\text{C}$  and then cooled to  $-70^\circ\text{C}$ . The resonance due to (py) $\text{TTPFe}^{\text{IV}}=\text{O}$  has been lost from the spectrum.

The characteristic pyridine resonances of (py) $\text{TTPFe}^{\text{IV}}=\text{O}$  can

(33) Chin, D. H.; Balch, A. L.; La Mar, G. N. *J. Am. Chem. Soc.* **1980**, *102*, 1446.

(34) La Mar, G. N.; de Ropp, J. S.; Latos-Grazynski, L.; Balch, A. L.; Johnson, R. B.; Smith, K. M.; Parish, D. W.; Cheng, R.-J. *J. Am. Chem. Soc.* **1983**, *105*, 782.

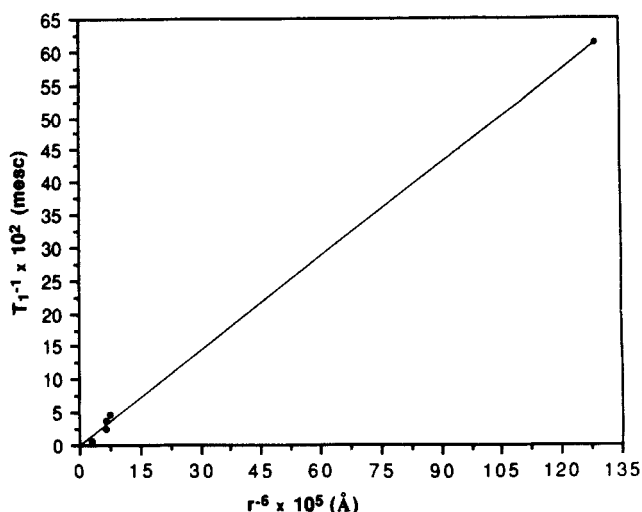


Figure 8. A plot of  $T_1^{-1}$  vs  $r^{-6}$  for  $\text{TTPFe}^{\text{III}}(1\text{-ad})$  in toluene- $d_8$  at  $-60^\circ\text{C}$ .

also be observed during this process, and these give further assurance of its formation. Figure 7 shows the  $^1\text{H}$  NMR spectrum of a sample of  $\text{TTPFe}(4\text{-cam})$  in toluene at  $-70^\circ\text{C}$  to which dioxygen and pyridine have been added successively. Trace A shows the portion of the spectrum upfield of TMS immediately after preparation. It should be compared with the spectrum of (py)TmTPFe $^{\text{IV}}=\text{O}$  shown in trace 1 of Figure 1 of ref 34. The two resonances seen are due to para protons of pyridine at  $-6$  ppm and the ortho protons at  $-29$  ppm. Trace B shows the effect of warming the sample to  $25^\circ\text{C}$  and recooling to  $-70^\circ\text{C}$ . The pyridine resonances of (py)TTPFe $^{\text{IV}}=\text{O}$  are lost.

## Discussion

The data presented here show that low-spin iron(III) porphyrin complexes with axial tertiary alkyl ligands (1-ad and 4-cam) can be prepared and spectroscopically detected at room temperature. As with other iron(III) porphyrin alkyl complexes, these are sensitive to light and reactive toward dioxygen.<sup>3</sup> Homolysis of the Fe-C bond appears to be particularly facile for the 1-ad derivative which in our preparations always is found in the presence of significant amounts of PFe $^{\text{II}}$ . In this respect, PFe $^{\text{III}}(1\text{-ad})$  resembles its benzyl analogue which also undergoes ready loss of the benzyl radical to form PFe $^{\text{II}}$ .<sup>3</sup>  $\text{TTPFe}^{\text{III}}(t\text{-Bu})$  can also be prepared and detected at low temperature, but it decomposes to  $\text{TTPFe}^{\text{II}}$  when warmed above  $0^\circ\text{C}$ . Studies of low-spin  $d^6$  cobalt(III) alkyl complexes, *trans*-alkylbis(dimethylglyoximate)-(N-methylimidazole)cobalt(III), have shown a remarkable lengthening of the Co-Co bond in the adamantyl complex (Co-C(1-ad), 2.154 (5) Å vs Co-C(methyl) 2.009 (7) Å) due to the steric constraints imposed by the 1-ad ligand.<sup>35,36</sup> It is very likely that these iron(III) tertiary alkyl complexes suffer from similar steric effects so that the Fe-C bonds are elongated and hence more readily susceptible to homolysis.

Recent work by Lexa, Savéant, and co-workers has presented electrochemical evidence for the formation of sterically encumbered alkyl complexes of iron porphyrins.<sup>37</sup> Their work showed evidence for the formation of *tert*-butyl complexes in four oxidations, Fe $^{\text{I}}$ , Fe $^{\text{II}}$ , Fe $^{\text{III}}$ , and Fe $^{\text{IV}}$ , and indicated that the Fe $^{\text{III}}$  form had very limited stability. Our observations on  $\text{TTPFe}^{\text{III}}(t\text{-Bu})$  are entirely consistent with their findings.

**NMR Characteristics of Axial Alkyl Ligands. 1. Relaxation Properties.** The assumption of metal-centered paramagnetic

Table III. Separation of Chemical Shifts into Contact and Dipolar Contributions for  $\text{TTPFe}^{\text{III}}(1\text{-ad})$ (toluene- $d_8$  at  $21^\circ\text{C}$ )

proton	$(\Delta H/H)^{\text{obs}}$	$(\Delta H/H)^{\text{iso}}$	GF <sup>a</sup>	$(\Delta H/H)^{\text{dip}}$	$(\Delta H/H)^{\text{con}}$
$\beta$	-19.85	-17.94	$2.74 \times 10^{-2}$	47.0	-64.9
$\gamma$	-14.37	-14.69	$1.08 \times 10^{-2}$	18.7	-33.4
$\delta$	-20.73	-21.38	$9.57 \times 10^{-3}$	16.6	-37.9
$\delta'$	10.21	9.892	$1.11 \times 10^{-2}$	19.1	-9.2
pyrr	-18.20	-27.24	$-6.9 \times 10^{-3}$	-11.8	-15.4

<sup>a</sup> Relative geometric factors  $(3 \cos^2 \theta - 1) r^{-3}$  using Fe-C distance of 2.0 Å and the structural data from ref 39.

relaxation yields to the anticipation that the  $T_1$  values for the various protons will be proportional to  $R_i^{-6}$  where  $R_i$  is the distance from the iron to the proton in question.<sup>38</sup> This allows for the complete assignment of the 1-ad resonances in  $\text{TTPFe}^{\text{III}}(1\text{-ad})$  by differentiating between the  $\delta$  and  $\delta'$  resonances. The upfield resonance ( $-21$  ppm  $25^\circ\text{C}$ ) has a much larger  $T_1$  than the downfield counterpart (10 ppm  $25^\circ\text{C}$ ), and so it must arise from the  $\delta$  protons and the downfield resonance must come from the  $\delta'$  protons. By using this assignment, Figure 8 shows a plot of the observed  $T_1$  data for  $\text{TTPFe}^{\text{III}}(1\text{-ad})$  versus  $R_i^{-6}$ .  $R_i$  values have been estimated for an Fe-C bond length of 2.0 Å with the iron 0.25 out of the porphyrin plane through the use of a set of crystallographically determined adamantyl coordinates.<sup>39</sup> The agreement shown in this figure substantiates the full assignment which, except for the  $\delta$ ,  $\delta'$  differentiation, rests on other factors. Comparison of the  $T_1$  data with the observed spectral line widths indicates that the line widths are proportional to  $T_1$ ; consequently, chemical exchange is not contributing to the line widths. The  $T_1$  data for  $\text{TTPFe}^{\text{III}}(4\text{-cam})$  also support the assignment of these resonances.

**2. Chemical Shifts.** The rigid, well-defined geometry of the adamantyl group provides an exceptionally good beginning for analyzing the factors responsible for determining the NMR spectral behavior of the alkyl complexes. The observed hyperfine shift,  $(\Delta H/H)^{\text{hf}}$ , is a composite of the dipolar shift,  $(\Delta H/H)^{\text{dip}}$ , and the contact shift,  $(\Delta H/H)^{\text{con}}$ , which reflects spin delocalization:<sup>40</sup>

$$(\Delta H/H)^{\text{iso}} = (\Delta H/H)^{\text{con}} + (\Delta H/H)^{\text{dip}}$$

The dipolar shift for axial symmetry is given by

$$(\Delta H/H)^{\text{dip}} = \frac{\beta^2 S(S+1)}{9kT} (g_{\parallel}^2 - g_{\perp}^2) [3 \cos^2 \theta - 1] / r^3$$

The dipolar contribution for the various protons can be assessed by assuming (as done for other low-spin iron(III) porphyrins<sup>28</sup>) that the hyperfine shift observed for the phenyl protons arises strictly from a dipolar contribution. These phenyl groups are assumed to have their planes oriented perpendicular to the porphyrin plane. This orientation isolates the two  $\pi$ -systems and limits  $\pi$ -spin transfer to the phenyls. The iron may be expected to lie out of the porphyrin plane toward the side of the alkyl group.<sup>41</sup> For  $\text{TTPFe}^{\text{III}}(1\text{-ad})$  the best fit of the phenyl hyperfine shifts with the calculated geometric factors,  $[3 \cos^2 \theta - 1] / r^3$  (where  $r$  is the iron-to-proton distance and  $\theta$  is the angle between the proton-iron vector and the  $z$  axis), occurs with the iron 0.25 Å out of the porphyrin plane. Utilizing this analysis, it is then possible to compute the geometric factors for the adamantyl group (with the Fe-C bond assumed to be 2.0 Å long and using a crystallographically established adamantyl structure<sup>39</sup>) and to separate the adamantyl hyperfine shifts into dipolar and contact terms. These shifts, computed from data taken at  $21^\circ\text{C}$ , are given in

(38) Swift, T. J. In *NMR of Paramagnetic Molecules*; La Mar, G. N., Horrocks, W. D., Jr., Holm, R. H., Eds.; Academic Press: New York, 1973; p 53-83.

(39) Pestana, D. M.; Power, P. P. *J. Am. Chem. Soc.* **1989**, *111*, 6887; structure of [(1-ad)PB(mesityl)]<sub>2</sub>.

(40) Jesson, J. P. In *NMR of Paramagnetic Molecules*; La Mar, G. N., Horrocks, W. D., Jr., Holm, R. H., Eds.; Academic Press: New York, 1973; pp 1-52.

(41) For  $\text{TTPFe}^{\text{III}}\text{Ph}$  the Fe-C distance is 1.955 (3) Å, and the iron is 0.17 Å out of the porphyrin plane. Doppelt, P. *Inorg. Chem.* **1984**, *23*, 4009.

(35) Bresciani-Pahor, N.; Marzilli, L. G.; Randaccio, L.; Toscano, P. J.; Zangrando, E. *J. Chem. Soc., Chem. Commun.* **1984**, 1508.

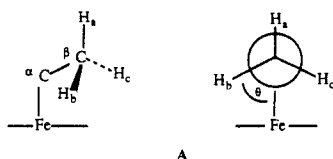
(36) Bresciani-Pahor, N.; Randaccio, L.; Zangrando, E.; Summers, M. F.; Ramsden, J. H., Jr.; Marzilli, P. A.; Marzilli, L. G. *Organometallics* **1985**, *4*, 2086.

(37) Gueutin, C.; Lexa, D.; Savéant, J.-M.; Wang, D.-L. *Organometallics* **1989**, *8*, 1607.

Table III. The dipolar shifts are quite large. Similarly large, dipolar shifts have been seen for low-spin aryl iron(III) porphyrin complexes.<sup>42</sup> After separating these, the contact shifts are all in the same direction: upfield. The relative ratio of shifts  $\beta/\gamma/\delta/\delta'$  observed for TTPFe<sup>III</sup>(1-ad) (1/0.51/0.15/0.58) is close in pattern to those observed for azaadamantane coordinated to nickel(II) where the ratio is 1/0.77/0.02/0.30.<sup>43</sup> The implication is that the mode of spin delocalization in the two saturated ligands with related geometry is similar, as would be expected. However, for the d<sup>8</sup> Ni(II) coordination, the shifts are all in the opposite direction, that is, downfield. This is also entirely reasonable and, indeed, opposite signs for spin density transfer to ligands have been predicted for d<sup>8</sup> and low-spin d<sup>5</sup> complexes.<sup>44</sup>

Similar considerations hold for the chemical shift patterns of the other alkyl complexes. The dipolar shifts expected for  $\beta$  and  $\gamma$  protons, in general, can be roughly estimated from the adamantyl data in Table III. Correcting for the large dipolar shifts results in upfield contact shifts for all the alkyl protons within the range of alkyl groups considered in Table I.

The protons of a  $\beta$ -methyl group on an axial alkyl ligand show an unusually large upfield hyperfine shift which may be considered as a diagnostic feature of this functional group. Thus the  $\beta$ -methyl resonances of the ethyl, isopropyl, and the *tert*-butyl groups have characteristic resonances at ca. -115 ppm (at 20 °C), whereas the  $\beta$ -methylene groups of the *n*-propyl, *n*-butyl, 1-ad, and 4-cam ligands appear at least 50 ppm downfield of these. This behavior is not unexpected. It is known that the <sup>1</sup>H contact shifts, like coupling constants in diamagnetic compounds, are sensitive to conformation. Consider the idealized C <sub>$\alpha$</sub> -C <sub>$\beta$</sub>  rotomer, A, shown below:



For  $\sigma$ -transmission of spin density, the contact shift is proportional to  $\cos^2 \theta$ , where  $\theta$  is the dihedral angle between the HCC and CCF<sub>e</sub> planes by<sup>45</sup>

$$\frac{A}{h} = (B_0 + B_2 \cos^2 \theta) \frac{\rho_c}{2S}$$

This relationship has had wide applicability to the study of the <sup>1</sup>H NMR spectra of paramagnetic complexes of aliphatic amines.<sup>43,46</sup> Consequently in A, H<sub>a</sub> is expected to have the largest contact shift of the three protons. For methyl groups in the  $\beta$ -position, all protons can occupy the H<sub>a</sub> position at some time, so long as free rotation occurs about the C <sub>$\alpha$</sub> -C <sub>$\beta$</sub>  bond. However, for methylene groups in the  $\beta$ -position, a carbon atom rather than a proton is more likely to occupy the site of H<sub>a</sub>. For the adamantyl group, of course, its rigid nature ensures that a carbon atom replaces H<sub>a</sub>. Thus at 20 °C the observed shift for the  $\beta$ -methylene protons is only -18.4 ppm. The *n*-propyl and *n*-butyl groups of methylene resonances are at higher fields than this simply because the methylene protons can move into the H<sub>a</sub> site, although that does produce unfavorable interactions between the porphyrin plane and the remaining part of the alkyl chain.

Comparison of the data for TTPFe(1-ad) with those for the

ethyl, isopropyl, and *tert*-butyl derivatives indicates that the contact shift for a proton restricted to the H<sub>a</sub> position is ca. -350 ppm (at 20 °C). In this analysis we assumed equal populations of the three sites (H<sub>a</sub>, H<sub>b</sub>, and H<sub>c</sub>) and used the observed shifts for the 1-ad derivative as fully representative of the equivalent H<sub>b</sub> and H<sub>c</sub> sites. For TTPFe<sup>III</sup>(4-cam), the difference in the chemical shift for the  $\beta_1$ - and  $\beta_2$ -protons also largely results from differences in  $\theta$  for these protons. Unlike the situation in the 1-ad derivative, for the 4-cam ligand the two methylene protons are inequivalent. Calculations show that 10° difference in  $\theta$  is sufficient to cause the observed chemical shift pattern.

The temperature dependence of the pyrrole and porphyrin phenyl resonances show behavior which is expected for low-spin iron(III) complexes. Thus the chemical shift for the pyrrole resonances give linear 1/T plots as shown in Figures 2 and 4 with extrapolated intercepts which are slightly downfield from the anticipated diamagnetic protons.<sup>28</sup> However, the axial alkyl resonances show anomalous behavior.<sup>47</sup> In particular the  $\beta$ -methyl resonances, while linear with 1/T, show intercepts that are far from the expected diamagnetic position and the  $\beta$ -methylene resonances for the isopropyl and 1-ad complexes show anti-Curie slopes over much of the temperature range available and pronounced curvature. These effects cannot be ascribed to anomalies in the dipolar shift contribution or to chemical exchange since the behavior of the pyrrole and phenyl resonances is normal. Rather, there must be some temperature effect operating on the contact term. This most likely involves the existence of different rotameric orientations of the alkyl group about the Fe-C bond which give the alkyl group differing orientations with regard to the porphyrin axes and different contributions to the contact shifts. Changes in the populations of these rotameric forms with temperature will produce differences in the temperature dependence of the hyperfine shifts. Notice that this anomaly is seen for the adamantyl derivative where geometric constraints limit the degrees of available motion of the ligand but do allow for motion about the Fe-C bond. Moreover, the equivalence of all  $\beta$ -protons for this derivative requires movement about that bond.

**Hydroperoxide Formation and Cleavage.** Dioxygen inserts into the Fe-C bonds of these three tertiary alkyl complexes under conditions similar to those used for the insertion into primary and secondary alkyl Fe-C bonds to produce the alkyl peroxide complexes. It is interesting to note that steric bulk on the alkyl group does not appear to retard insertion, while bulk on the porphyrin phenyl group does. Thus TTPFe(alkyl) and TPPFe(alkyl) undergo dioxygen insertion at a reasonable rate at -80 °C, but TMPFe-(CH<sub>3</sub>) requires warming to -50 °C to achieve a comparable rate of conversion to the alkyl peroxide complex.<sup>3</sup> This accords with the observation that ligands bind more strongly to and dissociate more slowly from a five-coordinated TMPFe(II)B than from a five-coordinated TPPFe(II)B.<sup>48</sup> This effect of other substituents on TPP properties has been attributed to steric hindrance toward porphyrin doming.<sup>48</sup>

The lack of  $\alpha$ -hydrogen atoms in these tertiary peroxide complexes was expected to alter the nature of the hydroperoxide decomposition step, since aldehyde or ketone formation via rapid hydrogen transfer from carbon to oxygen, eq 2, is not possible in these newly prepared derivatives. The spectra shown in Figures 6 and 7 establish that (py)PFe<sup>IV</sup>=O is formed upon addition of py to the peroxide complex (reaction 4). This observation con-

strasts with a similar experiment involving TTPFe<sup>III</sup>OO(Et).<sup>3</sup> In this case addition of 1-methylimidazole (1-MeIm) at -70 °C did not produce evidence for (1-MeIm)TTPFe<sup>IV</sup>=O, which had been spectroscopically observed independently,<sup>33,34</sup> but did show rapid formation of acetaldehyde. Thus without the  $\alpha$ -hydrogen present it is possible to detect an intermediate formed during alkyl peroxide

(42) Balch, A. L.; Renner, M. W. *Inorg. Chem.* **1986**, *25*, 303.

(43) Morishima, I.; Yoshikawa, K.; Okada, K. *J. Am. Chem. Soc.* **1976**, *98*, 3787. Morishima, I.; Okada, K.; Ohashi, M.; Yonezawa, T. *J. Chem. Soc., Chem. Commun.* **1971**, 33.

(44) La Mar, G. N. In *NMR of Paramagnetic Molecules*; La Mar, G. N., Horrocks, W. D., Jr., Holm, R. H., Eds.; Academic Press: New York, 1973; pp 85-126.

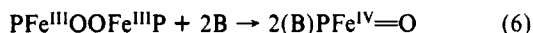
(45) Bertini, I.; Luchinat, C. *NMR of Paramagnetic Molecules in Biological Systems*; Benjamin/Cummings Publishing Co. Inc.: Menlo Park, CA, 1986; p 34. Pratt, L. *Disc. Faraday Soc.* **1962**, *34*, 88. Stone, E. W., Maki, A. H. *J. Chem. Phys.* **1962**, *37*, 1326.

(46) Zamarou, K. I.; Molin, Y. N.; Skwenuskaya, G. *J. Struct. Chem.* **1966**, *7*, 740. Ho, F. F. L.; Reilly, C. N. *Anal. Chem.* **1969**, *41*, 1835. Pratt, L.; Smith, B. B. *Trans. Faraday Soc.* **1969**, *65*, 915.

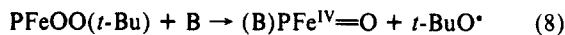
(47) Other cases of anomalous behavior of axial ligand resonances in porphyrin complexes are known. Arafa, I. M.; Goff, H. M.; David, S. S.; Murch, B. P.; Que, Jr., L. *Inorg. Chem.* **1987**, *26*, 2779.

(48) Portello, C. Ph.D. Thesis, University of California, San Diego, 1986.

breakdown. The direct detection of the ferryl complex is strong evidence for homolytic cleavage of the O–O bond of the alkyl peroxide complex in the nonpolar environment employed in this study. The six-coordinate ferryl complex has previously been obtained by two routes. It can be made from dioxygen via eqs 5 and 6.<sup>33,34,49</sup> Because of these reactions (5 and 6), samples



containing  $\text{TTPFe}^{\text{II}}$  are a source of the six-coordinate ferryl intermediate. Consequently, in searching for information regarding O–O bond cleavage, we restricted our presentation to data on  $\text{TTPFe}^{\text{III}}(4\text{-cam})$  where this complex could be prepared free from  $\text{TTPFe}^{\text{II}}$ . The six-coordinate ferryl complex can also be made from *tert*-butyl hydroperoxide via eqs 7 and 8.<sup>20</sup> The results



obtained here for insertion of dioxygen into the Fe–C bond of  $\text{TTPFe}^{\text{III}}(t\text{-Bu})$  are entirely consistent with the data obtained from earlier work on the reactions of *tert*-butyl hydroperoxide iron porphyrins in toluene.<sup>20</sup> Thus both routes (reactions 1 and 7) yield the same complex,  $\text{PFe}^{\text{III}}\text{OO}(t\text{-Bu})$ . All of the related processes 4, 6, and 8, result in homolytic cleavage and all are carried out in nonpolar media in which the formation of electrically neutral products is strongly favored.

### Experimental Section

**Materials.**  $\text{TTPH}_2$ ,<sup>50</sup> pyrrole- $d_8$ - $\text{TTPH}_2$ ,<sup>51</sup> and (tolyl- $d_{28}$ )- $\text{TTPH}_2$ <sup>52</sup> were prepared by reported procedures, and iron was inserted by the standard route.<sup>53</sup> Toluene (Fisher) was distilled over sodium under nitrogen, deoxygenated by three freeze–pump–thaw cycles and stored in a Vacuum Atmospheres glovebox. Ether (Fisher) was distilled over sodium/potassium amalgam under nitrogen. Cyclohexane (Fisher) was passed over 1 1/2 in. by 12 1/2 in. column of silica gel, distilled over calcium hydride under nitrogen and stored over sodium. Toluene- $d_8$  (Aldrich) was deoxygenated and stored in the glovebox. Fifty grams of basic alumina (Aldrich) was deoxygenated by placing it under vacuum in a

silicon oil bath at 150 °C for 2 h, cooling to 25 °C, and maintaining under vacuum for 3 days. *n*-Propyl, isopropyl, and *tert*-butyl magnesium bromides and 1-bromoadamantane were purchased from Aldrich Chemical Company. 4-Chlorocamphane was a 35-year-old specimen that had sublimed from the original preparation.<sup>22</sup> 300 MHz  $^1\text{H}$  NMR (in benzene- $d_6$ ) singlet (s) (6) 0.8 ppm, s(3) 0.68 ppm, multiplet (m) (2) 1.02 ppm, m(2), 1.3 ppm, m(2) 1.65 ppm and m(2) 1.9 ppm. Both the 1-bromoadamantane and 4-chlorocamphane were dried over sodium hydroxide pellets before use. Magnesium turnings were purchased from Fisher Chemical Company. Lithium wire (0.8% sodium) was purchased from Aldrich Chemical Company.

**Preparation of  $\text{TTPFe}^{\text{III}}(1\text{-ad})$ .** Adamantylmagnesium bromide was prepared in ethyl ether solution from magnesium and 1-bromoadamantane without stirring under the conditions of Molle et al.<sup>29</sup> A sample of 15–20 mg of  $\text{TTPFe}^{\text{III}}\text{Cl}$  was dissolved in 15–20 mL of dioxygen-free toluene, and a 1.4 molar quantity of deoxygenated adamantylmagnesium bromide in ethyl ether was added under subdued lighting. The solution immediately turned from green to red. After stirring for 5 min the entire sample was placed on a 13 mm × 26 mm column of basic alumina and eluted with toluene. The red fraction was collected and evaporated to dryness. Any newly formed  $\text{TTPFe}^{\text{III}}\text{OFe}^{\text{III}}\text{TTP}$  was retained near the top of the column. The solid  $\text{TTPFe}^{\text{III}}(1\text{-ad})$  was stored in a dinitrogen-filled glovebox in the dark and dissolved in toluene- $d_8$  for spectroscopic studies.

**Preparation of  $\text{TTPFe}^{\text{III}}(4\text{-cam})$ .** A cyclohexane solution of 4-camphyllithium was prepared from 4-chlorocamphane and lithium wire (0.8% sodium) according to the procedure of Traylor and Winstein.<sup>22</sup> This was added to  $\text{TTPFe}^{\text{III}}\text{Cl}$  as described above, and the iron complex was purified in the fashion presented earlier.

**Preparation of  $\text{TTPFe}^{\text{III}}(t\text{-Bu})$ .** A sample of 3 mg of  $\text{TTPFe}^{\text{III}}\text{Cl}$  was dissolved in 0.5 mL of dioxygen-free toluene- $d_8$  in a glovebox. The sample was placed in a 5-mm NMR tube, capped with a rubber septum, and sealed with Parafilm. The sample was cooled to –80 °C in a bath of dry ice and ethanol. One equivalent of *tert*-butylmagnesium chloride in diethyl ether was added to the NMR tube via a syringe under subdued lighting. The sample was shaken vigorously until the characteristic red color appeared. The sample was then immediately transferred to an NMR instrument, while its temperature was maintained at –80 °C.

**Oxygenations.** Reactions of  $\text{TTPFe}(1\text{-ad})$  and  $\text{TTPFe}(4\text{-cam})$  with dioxygen were performed as described previously.<sup>3</sup>

**Instrumentation.** NMR spectra were recorded on Nicolet NT-360 FT and NT-500 FT spectrometers operating in the quadrature mode ( $^1\text{H}$  frequencies are 360 and 500 MHz, respectively). Transients (500–2000) were collected in  $^1\text{H}$  NMR over a 40–60-kHz sweepwidth by using a delay time of 100 ms and a 5.25  $\mu\text{s}$  90° pulse. Transients (2000–10 000) were acquired in  $^2\text{H}$  NMR with a 15  $\mu\text{s}$  90° pulse, a delay time of 1 ms, and a sweepwidth of 10–15 kHz. The residual methyl peaks (2.09 ppm) of toluene- $d_8$  were used as a second reference.

**Acknowledgment.** We thank the National Institutes of Health (Grant GM-26226) for support, C. Cornman for a sample of *p*-tolyl- $d_{28}$ - $\text{TTPH}_2$ , and Dr. R. Arasasingham for helpful discussions.

(49) Chin, D. H.; La Mar, G. N.; Balch, A. L. *J. Am. Chem. Soc.* **1980**, *102*, 4344.

(50) Adler, A. D.; Longo, F. R.; Finarelli, J. D.; Goldmacher, J.; Assour, J.; Korsakoff, L. *J. Org. Chem.* **1967**, *32*, 476.

(51) Boersma, A. D.; Goff, H. M. *Inorg. Chem.* **1982**, *21*, 581.

(52) Balch, A. L.; Cornman, C. R.; Latos-Grazynski, L. To be published.

(53) Adler, A. D.; Longo, F. R.; Kampas, F.; Kim, J. *J. Inorg. Nucl. Chem.* **1970**, *32*, 2443.